Formation of the ordered array of Al magic clusters on Si(111)7×7

V. G. Kotlyar,[1] A. V. Zotov,[1,2] A. A. Saranin,[1,3] T. V. Kasyanova,[1] M. A. Cherevik,[3] I. V. Pisarenko,[1] and V. G. Lifshits[1,2,3]
[1]*Institute of Automation and Control Processes, 690041 Vladivostok, Russia*
[2]*Department of Electronics, Vladivostok State University of Economics and Service, 690600 Vladivostok, Russia*
[3]*Faculty of Physics and Engineering, Far Eastern State University, 690000 Vladivostok, Russia*
(Received 28 April 2002; published 2 October 2002)

Deposition of Al onto the Si(111)7×7 surface held at temperatures ranging from 475 to 600 °C has been found to result in the formation of a superlattice of the identical-size nanoclusters (magic clusters). The Al magic clusters appear to have the structure similar to that reported recently for the magic clusters of Ga and In on Si(111): each cluster contains six metal atoms linked by three Si atoms. The present results reveal that at the early stages of deposition all the group III metals demonstrate a distinct tendency for the formation of the magic clusters on Si surfaces.

DOI: 10.1103/PhysRevB.66.165401 PACS number(s): 68.35.Bs, 68.55.Jk

Self-organized formation of the ordered arrays of the identical-size nanoclusters (i.e., magic clusters) on the solid surfaces is a fabulous challenge of scientific and technological research. Recently the goal has been achieved by using the metal deposition onto the Si(111)7×7 surface.[1–3] Vitali, Ramsey, and Netzer[1] have found that upon room-temperature (RT) deposition of about 0.2 monolayer (ML) (1 ML=7.8 $\times 10^{14}$ cm^{-2}) of thallium (Tl) onto Si(111), Tl adatoms agglomerate into the nanoclusters of ~9 adatoms located in the faulted halves of the 7×7 unit cells (HUC's) thus forming a superlattice of Tl nanoclusters. Lai and Wang[2] reported ''an unprecedented two-dimensional lattice of magic clusters'' each built of exactly six gallium (Ga) atoms linked by three Si atoms and residing at the centers of both faulted and unfaulted 7×7 HUC's. Li *et al.*[3] have grown an ordered array of the identical-size indium (In) clusters ''by delicate regulation of the growth kinetics.'' It is particularly remarkable that magic clusters of In and Ga appear to have an identical structure.

One can notice that in all three cases the adsorbates were group-III metals. Two species are left, boron (B) and aluminum (Al). While B demonstrates adsorption properties very different from those of other group-III metals, Al behavior at the early stages of adsorption is very similar to that of In and Ga [e.g., formation of the same $\sqrt{3}\times\sqrt{3}$ structure on Si(111),[4,5] as well as the similar 2×3, 2×5, and 2×2 structures on Si(100) (Ref. 6)]. Thus one can expect the formation of the ordered arrays of the magic clusters in the Al/Si(111) system also. The early scanning tunneling microscopy (STM) observations of the so-called α-7×7 Al/Si(111) phase by Yoshimura *et al.*[7,8] provide additional promise to reach the goal. Indeed, the results of the present study reveals the formation of the ordered arrays of Al magic clusters on Si(111)7×7. The Al magic clusters have been shown to be identical to the In and Ga ones, indicating that their formation is a general phenomenon for group-III metals.

Our experiments were performed with Omicron STM operated in an ultrahigh vacuum ($\sim 1.5\times 10^{-10}$ Torr). Atomically clean Si(111)7×7 surfaces were prepared *in situ* by flashing to 1250 °C after the samples were first outgassed at 600 °C for several hours. Aluminum was deposited from a heated Al-cowered W wire at a typical deposition rate of ~0.3 ML/min. The samples were heated by passing dc current through them. For STM observations, electrochemically etched tungsten tips cleaned by *in situ* heating were employed. The STM images were acquired in a constant-current mode after cooling the sample to room temperature.

Formation of the highly ordered superlattice of the Al nanoclusters on the Si(111)7×7 surface is illustrated by Fig. 1, showing the surface after deposition of ~0.35 ML of Al at 575 °C. One can see that every 7×7 HUC is occupied by the identical-size triangle-shaped cluster. The cluster shows up as a group of three protrusions in the filled states [Fig. 2(a)] and as a group of six protrusions in the empty states [Fig. 2(b)]. This STM appearance of Al clusters coincides exactly with the STM appearance reported for the magic clusters of Ga and In adatoms.[2,3] The atomic structure of the magic clusters as elucidated by means of first-principles total energy calculations[3] is shown in Fig. 2(c). The structure was originally proposed for the Ga magic clusters formed on Si(111)$\sqrt{3}\times\sqrt{3}$-Ga reconstruction[9] and it consists of six metal atoms linked through three Si atoms to form a triangle-shaped configuration with satisfied bonding. The six protru-

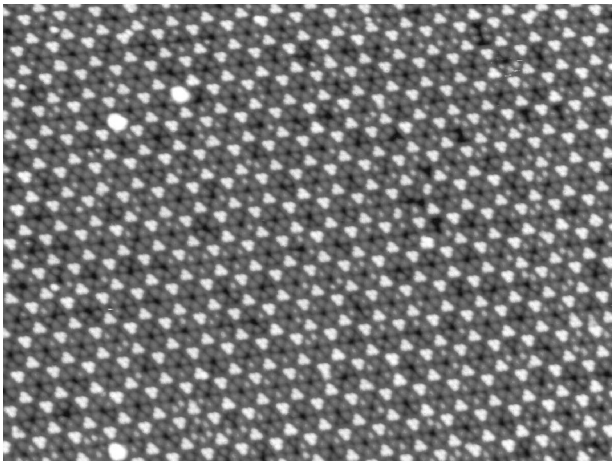

FIG. 1. Filled state (+2.0 V) STM image (470×320 Å^2) of the ordered array of the Al identical-size nanoclusters (magic clusters) formed by depositing ~0.35 ML onto the Si(111)7×7 surface held at 575 °C.

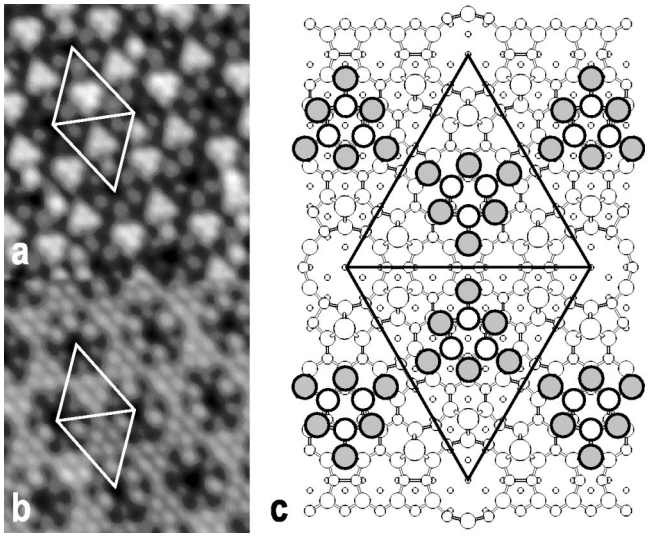

FIG. 2. (a) Filled state (+2.0 V) and (b) empty state (−2.0 V) STM appearance of the Al magic clusters. (c) Atomic structure of the magic cluster of the group-III metals, as established in Refs. 2,3, and 9. The magic cluster is built of six metal atoms (gray circles) linked through three top Si atoms. The protrusions seen in filled states correspond to the location of the top Si atoms, the protrusions seen in empty states to that of the metal atoms. The 7×7 unit cell is outlined.

sions seen in the empty-state STM images correspond to the location of metal atoms, the three protrusions seen in the filled-state STM images consequently to the location of the top Si atoms.

The magic cluster consumes three edge Si adatoms of the original Si(111)7×7 DAS structure and hence, in the ideal case, would preserve the original top Si atom density of 102/49≅2.08 ML's. However, the corner Si adatoms are also involved in the reaction with deposited Al and become partially replaced by Al atoms. In the empty states, the Al adatoms are seen as more bright [Fig. 3(a)], as revealed by comparison with the Si adatoms on the bare Si(111)7×7 surface. As one can see in Fig. 3(b), the released Si atoms agglomerate into the flat islands, having one atomic layer height and located along the 7×7 domain boundaries. As illustrated by the inset in Fig. 3(b), the island surface is covered mostly by the 7×7 superlattice of magic clusters with some inclusions of $\sqrt{3}\times\sqrt{3}$-Al and $\sqrt{7}\times\sqrt{7}$-Al reconstructions. In Fig. 3(b), the islands occupy ~0.04 of the surface area. As the islands have a thickness of one Si(111) bilayer (i.e., 2 ML's), they accumulate ~0.08 ML of Si. The direct counting of the substituted corner adatoms in the high-resolution STM images shows that of six corner Si adatoms per 7×7 unit cell 3–4 adatoms are replaced by Al adatoms, i.e., ~0.06–0.08 ML of Si is liberated, in reasonable agreement with the above estimation of Si amount accumulated in islands.

Discrimination between Si and Al adatoms allows the insight into the atomic-scale processes involved in the formation of the superlattice of magic Al clusters. There are three various adsorption sites for Al adatoms. First, Al adatom can be incorporated in the magic cluster (there are six such sites

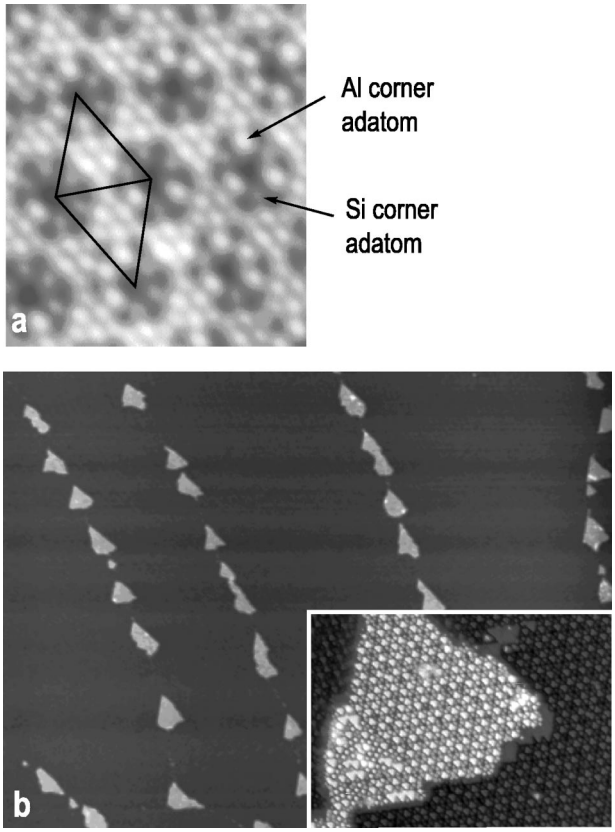

FIG. 3. (a) Empty state (−2.0 V) STM image (80×92 Å^2) of the 7×7 superlattice of Al magic clusters. The different contrast of the corner adatoms indicates that some of corner Si adatoms are substituted by Al atoms, which seen as more bright. (b) Large-scale (7000×5200 Å^2) topographic STM image showing the islands formed upon agglomeration of the displaced Si atoms. The islands have one atomic layer height. The inset shows the structure of the island top, which is basically the 7×7 superlattice of the Al magic clusters.

per 7×7 HUC). Second, Al adatom can substitute for the corner Si adatom (three sites per 7×7 HUC). Third, Al adatom can substitute for the edge Si adatom in the 7×7 HUC, which preserves the original DAS structure (three sites per 7×7 HUC). Variation in the occupation number for each site in the course of deposition is illustrated in Fig. 4. Three distinct stages can be distinguished, labeled I, II, and III.

At the stage I (below ~1.5 Al atoms per HUC, i.e., ≤0.06 ML of Al), formation of the magic clusters is a minor process and the most of deposited Al adatoms simply substitute for Si adatoms. The substitution of edge adatoms prevails over substitution of corner adatoms and the occupation of faulted HUC's prevails over occupation of unfaulted HUCs. The occupation numbers for respective sites are shown in a Table I. These data allow us to estimate the difference in activation energy for Al substitution of Si adatoms of various types by applying the Boltzmann distribution, $R=\exp(-\Delta E/kT)$, with R denoting the ratio of the occupation numbers of the respective sites at temperature $T=833$ K, ΔE the energy difference and k the Boltzmann constant. The results of estimation are summarized in Table I with the activation energy for substitution of the corner adatom in the faulted HUC as a reference point.

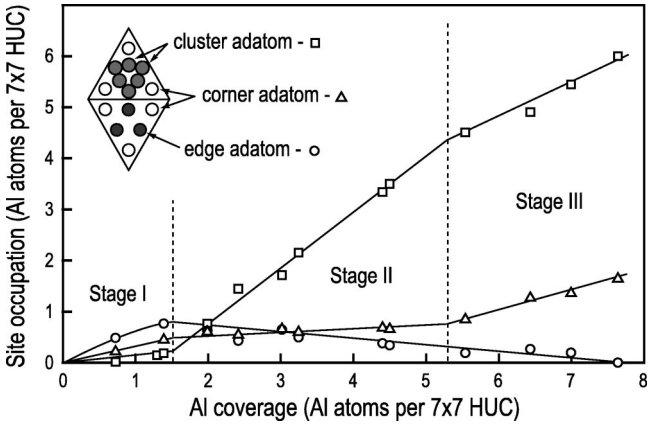

FIG. 4. Variation of the occupation numbers for the three adsorption sites, namely, in the magic clusters (open squares), in the edge adatom sites (open circles), in the corner adatom sites (open triangle), versus Al coverage. The occupation numbers and deposited Al coverage are expressed in the units of the mean number of Al atoms per 7×7 half unit cell (HUC). Three distinct stages are indicated. The growth temperature is 560 °C.

At the stage II (from ~1.5 to ~5 Al atoms per HUC, i.e., at 0.06–0.20 ML of Al), the growth of the magic clusters is the major process. Recall, that for the formation of each cluster, six Al adatoms and three Si adatoms are needed. The required number of Al atoms is get as a sum of the edge adatoms, substituted by Al at the initial stage, and arriving Al adatoms. Say, if all three edge adatoms in the HUC have been substituted by Al atoms, additional three Al adatoms have to be supplied by deposition. Supply of Si adatoms is another crucial process for the cluster formation. At the stage I, Si adatoms, expelled by Al atoms, agglomerate into islands and thus they cannot contribute to the subsequent cluster growth. At the stage II, the area occupied by islands has been found to remain practically unchanged, which means that most of the Si adatoms liberated upon Al substitution are involved in cluster formation. In other words, the growth of the cluster in a certain HUC takes place through the supply Si adatoms displaced from the neighboring HUC's. The main contribution comes from the substitution of the edge adatoms. The contribution from the Al substituted corner adatoms is not so essential as indicated by slow increase in their occupation number. The second stage is completed when about 75% of HUC's are occupied by the magic clusters.

TABLE I. Occupation number and estimated activation energy difference for Al substitution of Si adatoms in different sites at the early stage of Al deposition (~0.03 ML of Al) onto Si(111)7×7 surface held at 560 °C.

	Faulted 7×7 HUC		Unfaulted 7×7 HUC	
	Corner adatom	Edge adatom	Corner adatom	Edge adatom
Occupation number, atoms per 7×7 HUC	0.19	0.28	0.07	0.13
Activation energy difference, eV		−0.03±0.01	+0.08±0.01	+0.03±0.01

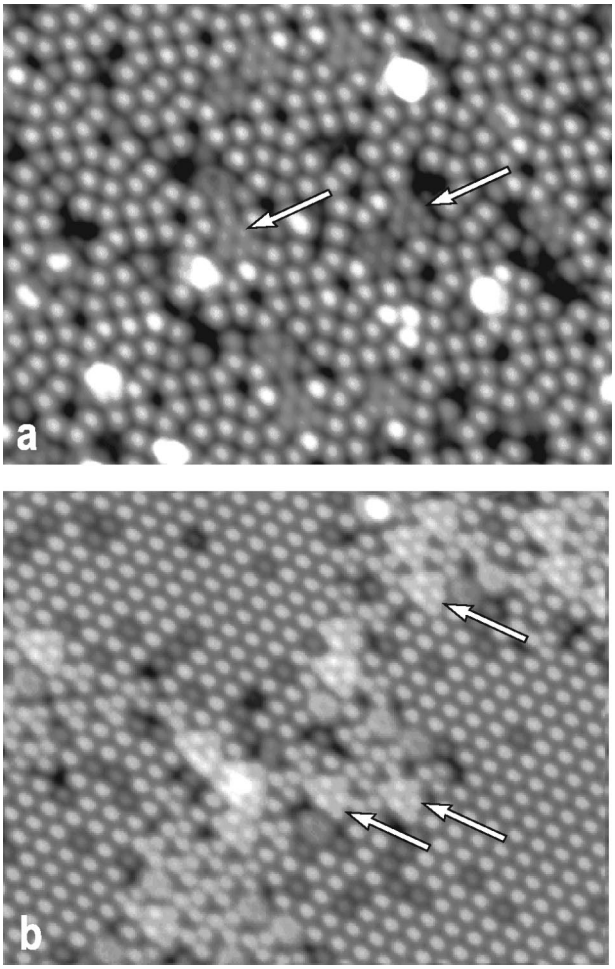

FIG. 5. The surface structure obtained at the temperatures out of the range, where the formation of perfect ordered array of Al magic clusters takes place. (a) Empty state (−1.0 V) STM image (190 ×130 Å^2) of the surface obtained by deposition of ~0.12 ML of Al onto the Si(111)7×7 surface held at 400 °C. Besides the formation of the magic clusters (indicated by arrows), the growth of the clusters of irregular shape takes place. (b) Empty state (−2.0 V) STM image (180×145 Å^2) of the surface obtained by annealing of the ordered array of magic clusters as shown in Fig. 1 to 750 °C. The surface comprises the $\sqrt{3}\times\sqrt{3}$-Al reconstruction with inclusions of the $\sqrt{7}\times\sqrt{7}$-Al reconstruction. Along the boundaries between two reconstructions, the magic clusters are seen (indicated by arrows).

At the stage III (from ~5 to ~8 Al atoms per HUC, i.e., at 0.20–0.33 ML of Al), all the left HUCs become filled by the magic clusters. As the edge adatoms as a source of Si adatoms have been already exhausted at the stage II, the Si adatoms are mostly supplied by the Al substitution of the corner adatoms. As a result, the number of the Al substituted corner adatoms increases rapidly, so that eventually about half of the corner adatom sites become occupied by Al atoms.

Formation of the ordered array of perfect Al magic clus-

ters takes place at temperatures ranging from 475 to 600 °C. Below 475 °C, the growth of magic clusters is accompanied by the formation of the clusters of irregular shape [Fig. 5(a)]. Upon annealing to temperatures above 600 °C, the array of magic clusters become thermally unstable and the surface evolves eventually to the $\sqrt{3}\times\sqrt{3}$-Al reconstruction with some inclusions of the $\sqrt{7}\times\sqrt{7}$-Al reconstruction. Note that the magic clusters still occur at the boundaries between the two reconstructions. All the magic clusters are in a single orientation, since the stacking faults of original 7×7 surface have been removed upon high-temperature annealing. The spacing between magic clusters has nothing with the original 7×7 periodicity, which means that they are newly formed ones rather than those left from the original ordered array of magic clusters.

In conclusion, the results of present work for the Al/Si(111) system in conjunction with the published data for the Tl/Si(111),[1] Ga/Si(111),[2] and In/Si(111) (Ref. 3) show that all of the above group-III metals demonstrate a similar tendency towards the formation of the magic clusters at the initial stages of adsorption (below about 0.3 ML). It is remarkable, that the growth of group-III metals on Si(100) surface presents also the vivid examples of the magic cluster formation: Upon deposition of up to 0.2 ML of Al onto the Si(100) surface held at 400–600 °C, the Al clusters are formed[10–12] having identical size (presumably, of eight Al atoms[13]). The Al clusters exhibit identical shape, but their spatial distribution on the surface is random. At In growth on Si(100) at 300–400 °C, the magic clusters are formed built of seven In atoms and six Si atoms.[14] At the early stages of deposition, their spatial distribution is almost random, but with increasing In coverage they become arranged into the well-ordered Si(100)4×3 superlattice. The list of examples can be continued by other group-III magic-size objects. For instance, Fig. 6 shows the identical-size $\sqrt{3}\times\sqrt{3}$-Al patches containing six Al adatoms embedded in the extended array of

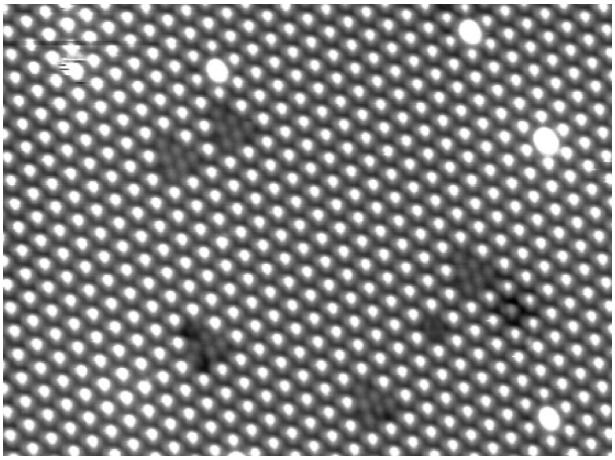

FIG. 6. Filled state (+2.4 V) STM image (265×190 Å^2) showing the magic-size patches of the $\sqrt{3}\times\sqrt{3}$-Al reconstruction containing six Al adatoms formed at the extended region of the $\sqrt{7}\times\sqrt{7}$-Al reconstruction.

$\sqrt{7}\times\sqrt{7}$-Al reconstruction. Taking into account that $\sqrt{3}\times\sqrt{3}$-Al has a lower Al coverage than $\sqrt{7}\times\sqrt{7}$-Al (1/3 ML versus 3/7 ML), these inclusions can be treated even as a kind of magic vacancy islands, which size selection is controlled by the relative orientation and periodicity of the two reconstructions. As a final remark, we would like to note that very recently a similar superlattice of Al magic clusters on Si(111)7×7 surface was independently obtained[15] by Jia *et al.*[15]

Part of this work was supported by Russian Foundation for Fundamental Researches (Grant No. 02-02-16105), by Program ''Universities of Russia'' (Grant No. UR.06.01.008), Russian Ministry of Industry and Science (Grant Nos. 40.012.1.1.1151 and 40.012.1.1.1178), and by FCP Program ''Integratsia'' (Grant No. A0026).

[1] L. Vitali, M.G. Ramsey, and F.P. Netzer, Phys. Rev. Lett. **83**, 316 (1999).
[2] M.Y. Lai and Y.L. Wang, Phys. Rev. B **64**, 241404 (2001).
[3] J.L. Li, J.F. Jia, X.J. Liang, X. Liu, J.Z. Wang, Q.K. Xue, Z.Q. Li, J.S. Tse, Z. Zhang, and S.B. Zhang, Phys. Rev. Lett. **88**, 066101 (2002).
[4] J.M. Nicholls, B. Reihl, and J.E. Northrup, Phys. Rev. B **35**, 4137 (1987).
[5] J. Zegenhagen, J.R. Patel, P.E. Freeland, D.M. Chen, J.A. Golovchenko, P. Bedrossian, and J.E. Northrup, Phys. Rev. B **39**, 1298 (1989).
[6] H.W. Yeom, T. Abukawa, M. Nakamura, S. Suzuki, S. Sato, K. Sakamoto, T. Sakamoto, and S. Kono, Surf. Sci. **341**, 328 (1995).
[7] M. Yoshimura, K. Takaoka, T. Yao, T. Sueyoshi, T. Sato, and M. Iwatsuki, J. Vac. Sci. Technol. B **12**, 2434 (1994).
[8] M. Yoshimura, K. Takaoka, T. Yao, T. Sato, T. Sueyoshi, and M. Iwatsuki, Phys. Rev. B **47**, 13 930 (1993).
[9] M.Y. Lai and Y.L. Wang, Phys. Rev. Lett. **81**, 164 (1998).
[10] T. Ichinokawa, H. Itoh, A. Schmid, D. Winau, and J. Kirschner, J. Vac. Sci. Technol. B **12**, 2070 (1994).
[11] N. Shimizu, H. Kitada, and O. Ueda, Phys. Rev. B **51**, 5550 (1995).
[12] C. Zhu, A. Kawazu, S. Misawa, and S. Tsukahara, Phys. Rev. B **59**, 9760 (1999).
[13] V. Kotlyar, A. Saranin, A. Zotov, V. Lifshits, O. Kubo, H. Ohnishi, M. Katayama, and K. Oura, Surf. Sci. **506**, 80 (2002).
[14] A.A. Saranin, A.V. Zotov, V.G. Lifshits, J.T. Ryu, O. Kubo, H. Tani, T. Harada, M. Katayama, and K. Oura, Phys. Rev. B **60**, 14 372 (1999).
[15] J. Jia, J.-Z. Wang, X. Liu, Q.-K. Xue, Z.-Q. Li, Y. Kawazoe, and S. Zhang, Appl. Phys. Lett. **80**, 3186 (2002).